



M2 macrophage-derived exosomal miR-145-5p protects against the hypoxia/reoxygenation-induced pyroptosis of cardiomyocytes by inhibiting TLR4 expression

Li Wei¹, Dongsheng Zhao²

¹Department of Electrocardiogram, The First People's Hospital of Nantong, Nantong, China; ²Department of Cardiology, The First People's Hospital of Nantong, Nantong, China

Contributions: (I) Conception and design: L Wei; (II) Administrative support: L Wei; (III) Provision of study materials or patients: D Zhao; (IV) Collection and assembly of data: L Wei; (V) Data analysis and interpretation: Both authors; (VI) Manuscript writing: Both authors; (VII) Final approval of manuscript: Both authors.

Correspondence to: Dongsheng Zhao, Department of Cardiology, The First People's Hospital of Nantong, No. 6 North Haierxiang, Chongchuan District, Nantong 226000, China. Email: ntyzds@163.com.

Background: Exosomes carrying micro ribonucleic acids (miRNAs) protect against myocardial ischemic injury. In the study, we sought to investigate the protective effect mechanism of M2 macrophage-derived exosome miR-145-5p in hypoxia-reoxygenation (H/R)-induced cardiomyocytes.

Methods: M2 macrophages were isolated and induced from blood donated by healthy donors. M2 macrophages were transfected with or without miR-145-5p. Exosomes derived from M2 macrophages were isolated and identified by flow cytometry, nanoparticle tracking analysis, and transmission electron microscopy (TEM). AC16 cells were used to establish an H/R model, and cell activity was detected using a Cell Counting Kit 8 (CCK-8). Western blot was used to detect the expression of gasdermin D (GSDMD), nucleotide-binding domain-like receptor protein 3 (NLRP3), and caspase-1 in the H/R-induced AC16 cells to evaluate pyroptosis. Immunofluorescence staining was used to detect the positive rates of PKH26 and caspase-1. Combined with database prediction, dual luciferase reporter assays were used to validate toll-like receptor 4 (TLR4) as a downstream target molecule of miR-145-5p. A real-time quantitative polymerase chain reaction (RT-qPCR) analysis and western blot were used to detect the expression of TLR4 in the AC16 cells.

Results: Flow cytometry, western blot, nanoparticle tracking and TEM results confirmed the successful isolation of M2 macrophage-derived exosomes. CCK-8 results showed M2 macrophage-derived exosomes decreased the viability of the H/R-induced cells. Western blot results showed the expressions of GSDMD, caspase-1, and NLRP3 were significantly downregulated in the H/R group. Moreover, CCK-8 results showed the M2 macrophage-derived exosome miR-145-5p significantly ameliorated H/R-induced AC16 cellular activity. Western blot results confirmed the expressions of GSDMD, NLRP3, and caspase-1 were significantly downregulated in the macrophage-derived exosome miR-145-5p group compared to the M2 macrophage-derived exosome NC (normal control) group. Immunofluorescence staining results displayed the same trend in terms of the caspase-1 positivity rate. Further, we demonstrated overexpression of TLR4 partially reversed the protective effect of M2 macrophage-derived exosome miR-145-5p in the H/R-induced AC16 cells. Additionally, overexpression of TLR4 reversed the protein expression associated with pyroptosis in M2 macrophage-derived exosome miR-145-5p in the H/R-induced AC16 cells.

Conclusions: Our study indicated M2 macrophage-derived exosomes carrying miR-145-5p inhibited H/R-induced cardiomyocyte pyroptosis by downregulating the expression of TLR4.

Keywords: Exosomes; miR-145-5p; pyroptosis; toll-like receptor 4 (TLR4); hypoxia/reoxygenation

Submitted Nov 01, 2022. Accepted for publication Dec 20, 2022.

doi: 10.21037/atm-22-6109

View this article at: <https://dx.doi.org/10.21037/atm-22-6109>

Introduction

Cardiovascular disease is currently the most common cause of death worldwide, and its morbidity and mortality rates continue to increase each year (1). Some studies (2) have predicted that the number of deaths due to cardiovascular disease could reach 22.2 million by 2030. Myocardial infarction, due to ischemia of the coronary vessels, leads to myocardial necrosis, and eventually heart failure and sudden death (3). Recently, research has shown (4) that prompt thrombolysis, percutaneous coronary intervention, and revascularization can save the infarcted myocardium and slow the course of the disease. However, blood supply restoration is accompanied by complex pathophysiological processes, including inflammatory factor release, oxidative stress, endothelial cell dysfunction, and energy metabolism imbalance, which can lead to myocardial tissue reperfusion injury (5,6). Currently, there are no effective therapeutic strategies to mitigate myocardial ischemia-reperfusion (I/R) injury. Thus, potential targeted therapeutic strategies that could, to some extent, reduce patient mortality need to urgently be explored.

I/R can induce various pathophysiological responses, including myocardial inflammatory responses. The inflammatory response promotes the progression of necrosis in the infarcted area; however, it is also involved in the regulation of damaged tissue repair (7). In addition to apoptosis, necrosis and autophagy, pyroptosis also plays a crucial role in myocardial I/R injury. NOD-like receptor protein 3 (NLRP3) inflammasome, as a participant in inflammatory immune response, is closely related to cardiovascular diseases (8). Zhang *et al.* reported (9)

that metformin could regulate the AMPK/NLRP3 inflammasome pathway, inhibit pyroptosis, and relieve the development of myocardial ischemia-reperfusion injury. Numerous studies have shown that activated M2 macrophages play a key role in the immune response and have an inhibitory effect on the development of myocardial infarction (10,11). Exosomes are extracellular vesicles of approximately 30–150 nm in diameter that can carry a variety of signaling molecules, such as proteins, micro ribonucleic acids (miRNAs) and RNAs (12,13). The exosomes that carry miRNAs play a signaling role, regulate multiple signaling pathways, and play a protective role in a variety of diseases (14,15).

Exosomes are vesicles with a diameter of 30 to 150 nm produced by a variety of cells, which have become important mediators of intercellular communication (16). It has been reported (17) that typical exosomes contain a large number of nucleic acids, proteins, lipids and miRNAs, which can regulate the function of recipient cells under various pathophysiological conditions. Much attention has been paid to the fact that exosomes carry miRNAs to regulate signaling between cells in tumors and cardiovascular diseases (18,19). Yang *et al.* reported (20) that exosomal miR-487a derived from M2 macrophages promotes gastric cancer progression by regulating T-cell intracellular antigen 1 (TIA1). Zhang *et al.* found (21) that exosomes derived from M2 macrophages carrying miR-21-5p promote renal cell carcinoma (RCC) cell invasion by the activation of the Phosphatase and TENsin homolog (PTEN)/protein kinase B (Akt) RCC cell signaling pathway. Long *et al.* suggested (22) that M2 exosomes carrying miR-1271-5p attenuate apoptosis in cardiomyocytes and promote cardiac repair by downregulating SRY-box containing gene 6 (SOX6) expression. An increasing number of studies have confirmed that exosome-carrying miRNAs inhibit disease progression, which suggests that exosome-carrying miRNAs may be a potential therapeutic strategy.

It has been shown (23) that in hyperlipidemia, miR-145-5p regulates lipid metabolism by targeting P21-activated kinase 7 and regulating the β -catenin signaling pathway. Zhou *et al.* reported (24) that the targeted regulation of apoptosis-inducing factor, mitochondrion-associated, 1 by miR-145-5p attenuates hypoxia-induced myocardial injury. However, the regulatory mechanism of the M2 macrophage-derived exosome miR-145-5p in myocardial I/R injury has not been examined.

In the present study, we focused on the effect of M2 macrophage-derived exosomes carrying miR-145-5p on hypoxia-reoxygenation (H/R)-induced cardiomyocyte

Highlight box

Key findings

- M2 macrophage-derived exosomal miR-145-5p protects against H/R-induced cardiomyocytes.

What is known and what is new

- miR-145-5p protects against H/R-induced cardiomyocytes.
- M2-macrophage-derived exosome miR-145-5p inhibits pyroptosis in H/R-induced cardiomyocytes by regulating the TLR4 expression.

What is the implication, and what should change now?

- Our study suggested that M2 macrophage derived exosomes carrying miR-145-5p could inhibit pyroptosis in H/R-induced cardiomyocytes, providing a potential new strategy for clinical treatment of myocardial injury.

injury. We showed that M2 macrophage-derived exosomes carrying miR-145-5p can target and regulate toll-like receptor 4 (TLR4) expression and play a protective role in cardiomyocyte injury. Additionally, our study found that miR-145-5p inhibited myocardial H/R-induced pyroptosis and attenuated cardiomyocyte injury. We present the following article in accordance with the MDAR reporting checklist (available at <https://atm.amegroups.com/article/view/10.21037/atm-22-6109/rc>).

Methods

Cell culture and cell transfection

Human AC16 cells (XY-XB-2181) were obtained from American Type Culture Collection (ATCC) and cultured in Dulbecco's Modified Eagle Medium (DMEM) containing 10% fetal bovine serum (FBS), and 1% streptomycin/penicillin. The AC16 cells were seeded in 6-well plates and incubated in a 37 °C incubator with 5% carbon dioxide (CO₂) at an appropriate humidity. The small-interfering RNA negative control (si-NC), miR-145-5p mimics, miR-145-5p inhibitor, TLR4-overexpressing lentiviral vector, and empty vector (NC) were designed and synthesized by Shanghai Sangon Biotech. Cell transfection was performed using Lipofectamine 3000 following the kit's instructions. After 48 h of transfection, the cells were collected for the subsequent experiments. The sequences of miR-145-5p mimics and miR-145-5p inhibitors were as follows: 5'-GUCCAGUUUCCCCA GGAAUCCCUGGAUCCUGGGAAAACUGGAC UU-3' and 5'-AGGGAUUCCUGGGAAAACUGGAC-3'. The negative control (miR-NC) was 5'-UUCUCCGAA CGUGUCACGUTT-3'.

Hypoxia/reoxygenation model

The AC16 cells were first cultured in DMEM (free of glucose and serum) and exposed to a humidified culture chamber with 95% nitrogen and 5% CO₂ for 12 h at 37 °C. Subsequently, the AC16 cells were transferred to DMEM containing 10% FBS and cultured for another 4 h.

Cell Counting Kit 8 (CCK-8)

Standardization was performed according to the instructions of the CCK-8. (Solarvio, CA1210). The absorbance value at a wavelength of 450 nm was detected using a microplate

reader to calculate the cell viability.

Western blot

We used ristocetin-induced platelet aggregation lysate to extract the protein from the AC16 cells, and we used a bicinchoninic acid assay kit (Solarbio, PC0020) to determine protein concentration. As previously reported (25), western blot was performed to detect the protein expression of the AC16 cells. The following primary antibodies were used: anti-CD9, anti-CD63 (Abcam, ab134045), anti-CD68 (Abcam, ab283316), anti-CD206 (Abcam, ab252921), anti-TSG101 (Tumor Susceptibility Gene 101) (Abcam, ab125011), anti-caspase-1 (Abcam, ab207802), anti-Gasdermin D (GSDMD) (Abcam, ab209845), anti-nucleotide-binding domain-like receptor protein 3 (NLRP3) (Abcam, ab264468), and anti-TLR4 (Abcam, ab13556).

Real-time quantitative polymerase chain reaction (RT-qPCR) analysis

As previously reported (26), TRIzol reagent was used to extract the total RNA from the AC16 cells. The complementary deoxyribonucleic acid (cDNA) was synthesized by reverse transcription using miScript RT II Buffer. The RT-qPCR was performed using the miScript HiSpec Buffer using an ABI7500 quantitative PCR instrument. The primers were synthesized and provided by Shanghai Sangon Biotech. The relative expression levels of miRNA/messenger RNA (mRNA) were calculated using the 2^{-ΔΔCT} method. Glyceraldehyde 3-phosphate dehydrogenase or U6 (small nuclear RNA) was used as the endogenous control. The following primers were used: miR-145-5p forward, TGTCCAGTTTTCCAGGAATC; reverse, CTCAACTGGTGTCTGGAGTC; TLR4 forward, 5'-AGT TGA TCT ACC AAG CCT TGA GT-3', reverse, 5'-GCTGGTTGTCCAAAATCACTTT-3'; U6, forward, CCT GCTTCGGCAGCACAT, reverse, AACGCTTCACGAATTTGCGT; GAPDH forward, 5'-TGTTTCGTTCATGGGTGTGAAC-3', reverse, 5'-ATGGCATGGACTGTGGTCAT-3'.

Dual luciferase reporter assays

Based on the database predictions, the binding site of miR-145-5p to TLR4 was cloned into a plasmid containing a dual luciferase reporter vector, which was provided by Shanghai GenePharma Co., Ltd. The TLR4-wt (wild

type)/mut (mutant type) with miR-145-5p mimics were co-transfected into the AC16 cells using Lipofectamine 3000. After 48 h of transfection, the relative luciferase activity was assayed according to the manufacturer's protocol.

Differentiation and polarization of macrophages

The monocytes were isolated from the peripheral blood of healthy donors. Using a previously reported method (27), isolated monocytes were cultured for 7 days to develop into M0 macrophages in a mixture of DMEM medium (Thermo) supplemented with 20 % FBS (Gibco), 1% penicillin/streptomycin (Gibco) and 100 ng/mL macrophage-colony-stimulating factor (M-CSF, Solarbio). Interleukin (IL)-4 (20 ng/mL) was then added to induce and simulate the activation in the M2 macrophages for 2 days. The positive rate and expression of CD68 and CD206 on the cell membrane surface were then detected by flow cytometry and western blot to identify the activated M2 macrophages. Our study was approved by the Hospital Ethics Committee and was conducted in accordance with the Declaration of Helsinki (as revised in 2013). The donors signed an informed consent form.

Exosome extraction and identification

The M2 macrophage culture medium was ultracentrifuged to obtain the exosomes. Briefly, the conditions for extraction were 500 ×g centrifugation for 10 min, followed by supernatantion at 3,000 ×g for 15 min, and further supernatantion at 140,000 ×g for 90 min to obtain the precipitate as the purified exosomes. Western blot was used to detect the expression of exosome specific marker (CD9, CD63, and TSG101) and identify the exosomes.

Nanoparticle tracking analysis

As previously reported (28), 30 µg of exosomes was dissolved in 1 mL phosphate buffered solution and vortexed for 30 s to mix well. The distribution sizes of the exosomes were analyzed by the NanoSight nanoparticle tracking analyzer.

TEM

The exosomes were observed by transmission electron microscopy (TEM). In brief (29), after being fixed with 4% paraformaldehyde, the exosomes were placed on Formvar

carbon-coated electron microscopy grids and fixed with 1% glutaraldehyde for 10 min. The samples were stained with a 2% solution of uranyl acetate. Finally, using a Tecnai transmission electron microscope, images of the exosomes were captured at 163 kV.

Hoechst 33342/propidium iodide (PI) staining

Hoechst 33342/PI staining was used to evaluate the pyroptosis-induced cell membrane damage. Briefly, AC16 cells were collected after H/R treatment, and Hoechst 33342 and PI staining solution were mixed. The cells were then incubated with Hoechst 33342/PI at 37 °C in the dark for 20 min. The nuclei were marked by Hoechst staining. Finally, the cells were observed under a fluorescence microscope and photographed.

Immunofluorescent staining

As described previously (30), the AC16 cells were fixed in 4% paraformaldehyde and permeabilized with 0.25% Triton X-100. Next, the AC16 cells were blocked with goat serum for 30 min at room temperature, incubated with a primary antibody (anti-caspase-1, or anti-PKH26) overnight at 4 °C. The next day, the cells were washed 3 times with phosphate-buffered saline (PBS) and then incubated with Immunoglobulin G secondary antibody for 1 h at room temperature. The nuclei were stained with 4',6-diamidino-2-phenylindole. Finally, the cells were randomly observed and photographed under a fluorescence microscope.

Statistical analysis

The data in the study are presented as the mean ± standard deviation. SPSS 22.0 statistical software package was used for the data analysis. The *in vitro* experiments were replicated 3 times. Comparisons between two groups were made using an independent-sample *t*-test, while comparisons between multiple groups were made using a univariate analysis of variance followed by Tukey's post-hoc test. P values <0.05 were considered statistically significant.

Results

Isolation and identification of M2 macrophage-derived exosomes

The M2 macrophages were isolated from peripheral blood

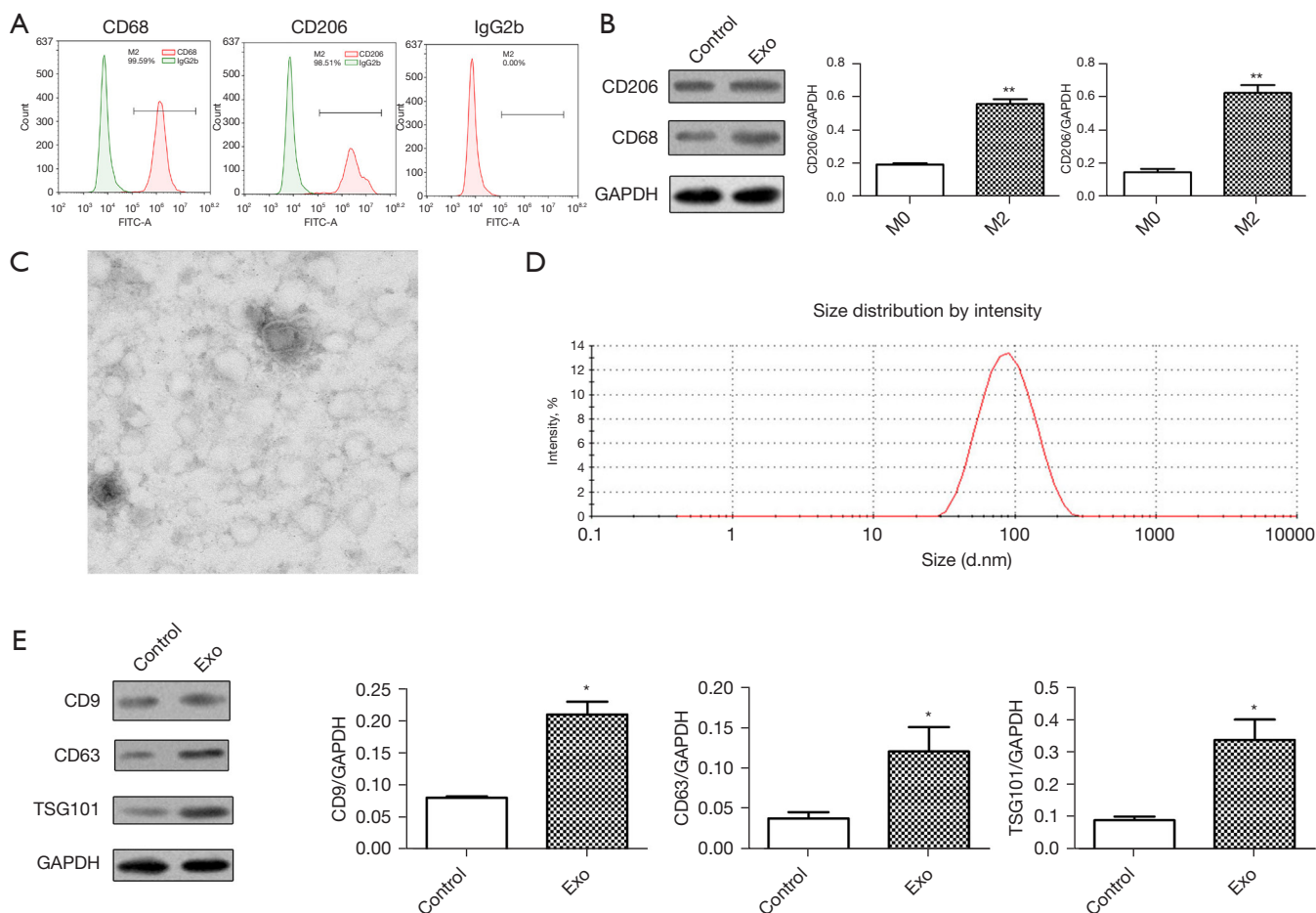


Figure 1 Isolation and identification of M2 macrophage-derived exosomes. (A) Flow cytometry was used to identify the exosomes derived from the M2 macrophages. (B) The expression of CD206 and CD68 in the exosomes was detected by western blot. (C) The exosomes were collected from the macrophage supernatants and observed using TEM (200,000 \times). (D) A nanoparticle tracking analysis was conducted to determine the particle sizes of the exosomes. (E) Western blot was used to detect the expression of CD9, CD63, and TSG101. * $P < 0.05$, ** $P < 0.01$, vs. control group. GAPDH, glyceraldehyde-3-phosphate dehydrogenase; TEM, transmission electron microscopy.

donated by healthy blood donors. First, the flow cytometry results (Figure 1A) revealed that the M2 macrophage markers CD68 and CD206 were positive. The western blot results (Figure 1B) confirmed that the protein expression of CD68 and CD206 was significantly upregulated in the M2 macrophages compared to the M0 macrophages, which confirmed the successful isolation and induction of M2 macrophages. To study the M2 macrophage-derived exosomes, nanoparticle tracking and TEM were used to analyze the size and morphology of the exosomes, respectively. The TEM results (Figure 1C) for the secretion showed that the exosomes had typical morphological features, including spherical structures formed by lipid

bilayers. The exosome particle size was approximately 100 nm (Figure 1D). The western blot results (Figure 1E) showed that the marker proteins (CD9, CD63, and TSG101) were significantly upregulated in the exosome group compared to the control group. The above results confirmed the successful isolation and induction of the exosomes derived from the M2 macrophages.

M2 exosomes protect against H/R-induced pyroptosis in AC16 cells

Next, we investigated the effects of M2 exosomes on H/R-induced pyroptosis in the AC16 cells. Immunofluorescence

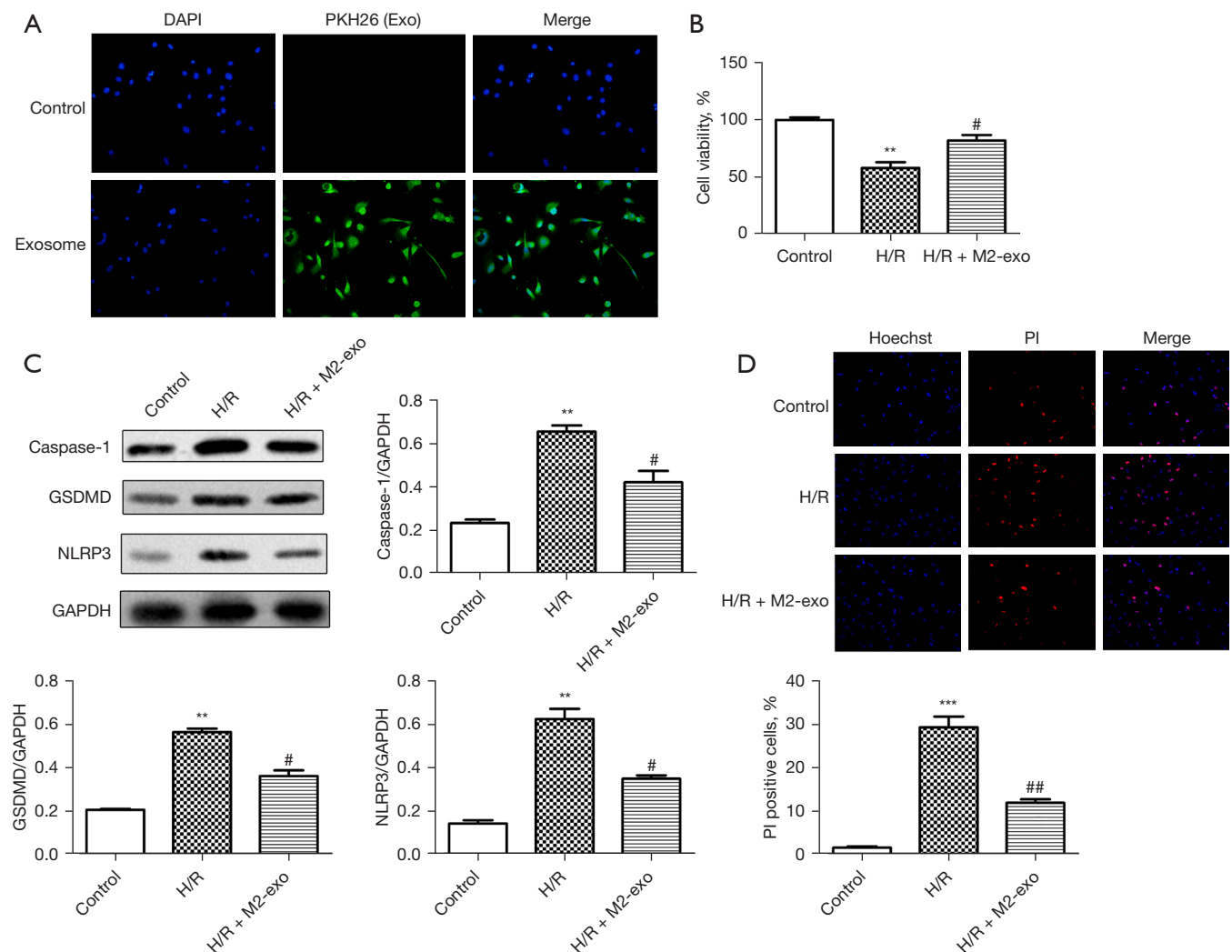


Figure 2 M2 exosomes protects against H/R-induced pyroptosis in AC16 cells. (A) The expression of PKH26 was detected by immunofluorescence staining (200 \times). (B) CCK-8 was used to detect cell viability. (C) The protein expression of caspase-1, GSDMD, and NLRP3 was detected using western blot. (D) PI staining was performed to detect pyroptosis. Nuclei were marked with Hoechst staining (blue). Necrotic cells were marked by PI staining (red), 100 \times . ** $P < 0.01$, *** $P < 0.001$, vs. control group. # $P < 0.05$, ## $P < 0.01$, vs. H/R group. NC, normal control; H/R, hypoxia-reoxygenation; PI, propidium iodide; GAPDH, glyceraldehyde-3-phosphate dehydrogenase; CCK-8, Cell Counting Kit 8.

staining (Figure 2A) showed that PKH26 positivity was more pronounced in the exosome group compared to the control group, revealing that AC16 cells could absorb exosomes from the M2 macrophages. The CCK-8 assay results (Figure 2B) showed that cell viability was partially restored in the H/R + M2 exosome group relative to the H/R group. The western blot results (Figure 2C) showed that the expression of caspase-1, GSDMD, and NLRP3 was significantly upregulated in H/R group compared to

the control group. After co-culture with M2 exosomes, the expression of caspase-1, GSDMD, and NLRP3 in the AC16 cells was significantly decreased. Additionally, the immunofluorescence staining results (Figure 2D) confirmed a significant increase in PI positivity in the H/R group cells; however, the PI positivity in the AC16 cells decreased in H/R+M2-Exo group compared to the H/R group. The results confirmed that M2 exosomes protected against H/R-induced pyroptosis in the AC16 cells.

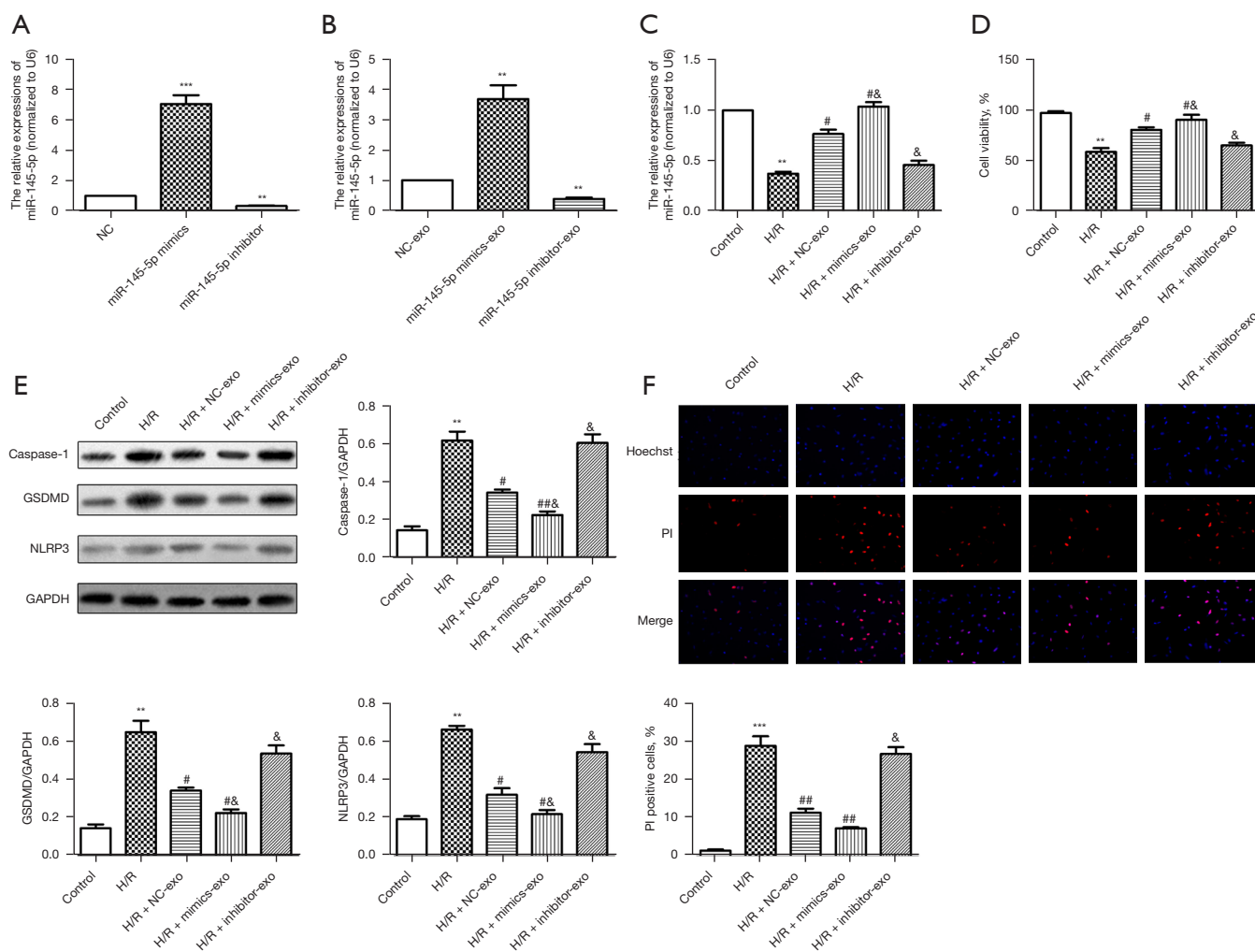


Figure 3 Exosomal transfer of miR-145-5p protects against H/R-induced pyroptosis in AC16 cells. (A-C) A RT-qPCR analysis was used to detect the levels of miR-145-5p. (D) CCK-8 was used to detect cell viability. (E) Western blot was used to detect the expression of caspase-1, GSDMD, and NLRP3 in the cells. (F) PI staining was used to detect pyroptosis. Nuclei were marked with Hoechst staining (blue). Necrotic cells were marked by PI staining (red), 100 \times . ** $P < 0.01$, *** $P < 0.001$, vs. NC/NC-exosome/control group; # $P < 0.05$, ## $P < 0.01$, vs. miR-145-5p mimic-exosome/H/R group; & $P < 0.05$, vs. H/R + mimic-exosome group. NC, normal control; H/R, hypoxia-reoxygenation; PI, propidium iodide; GAPDH, glyceraldehyde-3-phosphate dehydrogenase; RT-qPCR, real-time quantitative polymerase chain reaction; CCK-8, Cell Counting Kit 8.

MiR-145-5p exosomal transfer protects against H/R-induced pyroptosis in AC16 cells

Exosomes may be involved in the regulation of cell-to-cell interactions and the delivery of signaling proteins, RNAs, and miRNAs. Exosome-carrying miRNAs have been reported (31) to target the regulation of myocardial I/R-induced cardiomyocyte injury. In this study, we analyzed the role of exosome-carrying miR-145-5p in H/R-induced cardiomyocyte injury. The RT-qPCR results (Figure 3A)

showed that compared to the NC group, the expression of miR-145-5p was significantly increased in the miR-145-5p mimic group, while the expression of miR-145-5p was significantly decreased in the miR-145-5p inhibitor group. Similarly, after co-culture with exosomes, the RT-qPCR results (Figure 3B) displayed the same trend. Additionally, the RT-qPCR results (Figure 3C) showed that compared to the H/R group, the expression of miR-145-5p was significantly increased in the H/R + NC-exosome group. Compared to

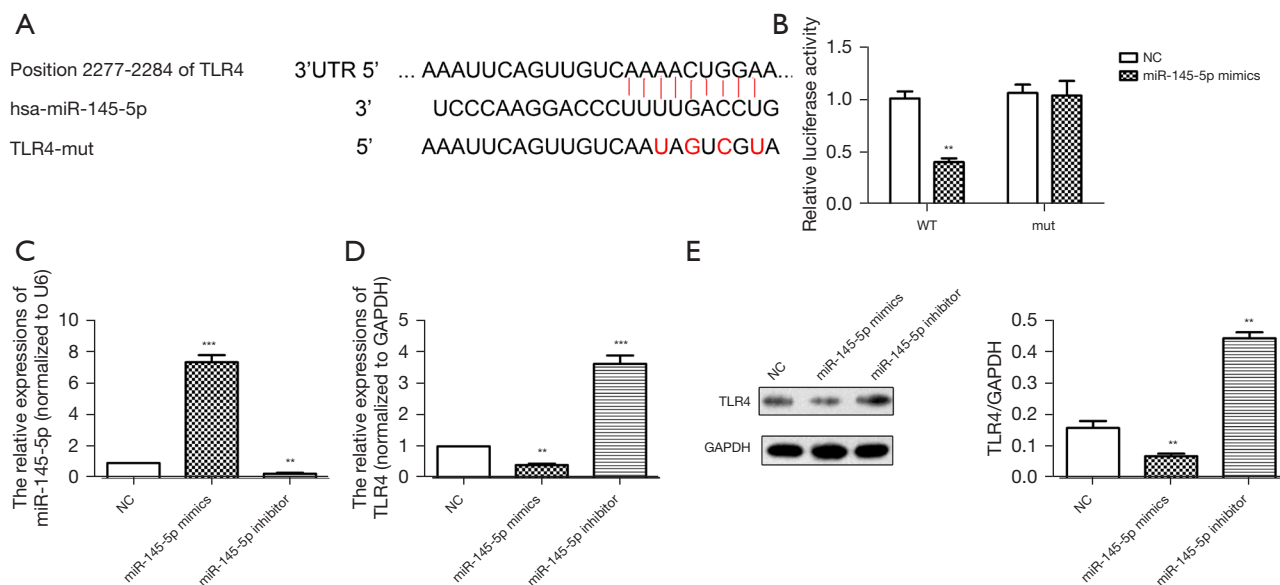


Figure 4 TLR4 was a potential target of miR-145-5p. (A) The predicted binding sites of miR-145-5p and TLR4. (B) Dual luciferase reporter assays verified the targeted binding of miR-145-5p to TLR4. (C) RT-qPCR analysis was used to detect the expression of miR-145-5p. (D) RT-qPCR analysis and western blot (E) were used to detect the expression of mRNA and protein of TLR4. ** $P < 0.01$, *** $P < 0.001$, *vs.* NC group; TLR4, toll-like receptor 4; NC, normal control; WT, wild type; mut, mutant type; GAPDH, glyceraldehyde-3-phosphate dehydrogenase; RT-qPCR, real-time quantitative polymerase chain reaction.

the H/R + NC-exosome group, the expression of miR-145-5p was significantly increased in the H/R + mimic-exosome group and decreased in the H/R + inhibitor-exosome group. As *Figure 3D* shows, cell viability was significantly increased in the H/R + NC-exosome group compared to the H/R group. Compared to the H/R + NC-exosome group, cell viability was significantly increased in the H/R + mimic-exosome group and decreased in the H/R + inhibitor-exosome group. The western blot results (*Figure 3E*) showed that the expression of caspase-1, GSDMD, and NLRP3 was significantly downregulated in the H/R + mimic-exosome group compared to the H/R + NC-exosome group, but significantly upregulated in the H/R + inhibitor-exosome group. The immunofluorescence staining results (*Figure 3F*) showed that the PI positive rate was higher in the H/R + mimic-exosome group than the H/R + NC-exosome group, while, the H/R + inhibitor-exosome group had less positivity. Taken together, we hypothesized that the exosomal transfer of miR-145-5p protects AC16 cells from H/R-induced pyroptosis.

TLR4 was a potential target of miR-145-5p

To identify the target genes regulated by miR-145-5p, we

used bioinformatics databases to predict the binding sites between miR-145-5p and TLR4 (*Figure 4A*). The dual luciferase gene report assay results (*Figure 4B*) confirmed the binding relationship between miR-145-5p and TLR4. Compared to the WT + NC group, the relative luciferase activity of the WT + miR-145-5p mimic group was significantly decreased. The RT-qPCR results (*Figure 4C*) showed that compared to NC group, the expression of miR-145-5p was significantly increased in the miR-145-5p mimic group, while the expression of miR-145-5p was significantly decreased in the miR-145-5p inhibitor group. As *Figure 4D* shows, compared to the NC group, the mRNA expression of TLR4 was significantly decreased in the miR-145-5p mimic group; however, it was significantly upregulated in the miR-145-5p inhibitor group. Similarly, the western blot results (*Figure 4E*) displayed the same trend. Thus, we confirmed TLR4 was a potential target of miR-145-5p.

TLR4 overexpression reversed the protective effects of M2 exosomes in H/R-induced pyroptosis

We also investigated the effect of TLR4 on M2 exosomes in H/R-induced pyroptosis. The western blot results (*Figure 5A*) showed that compared to the control group,

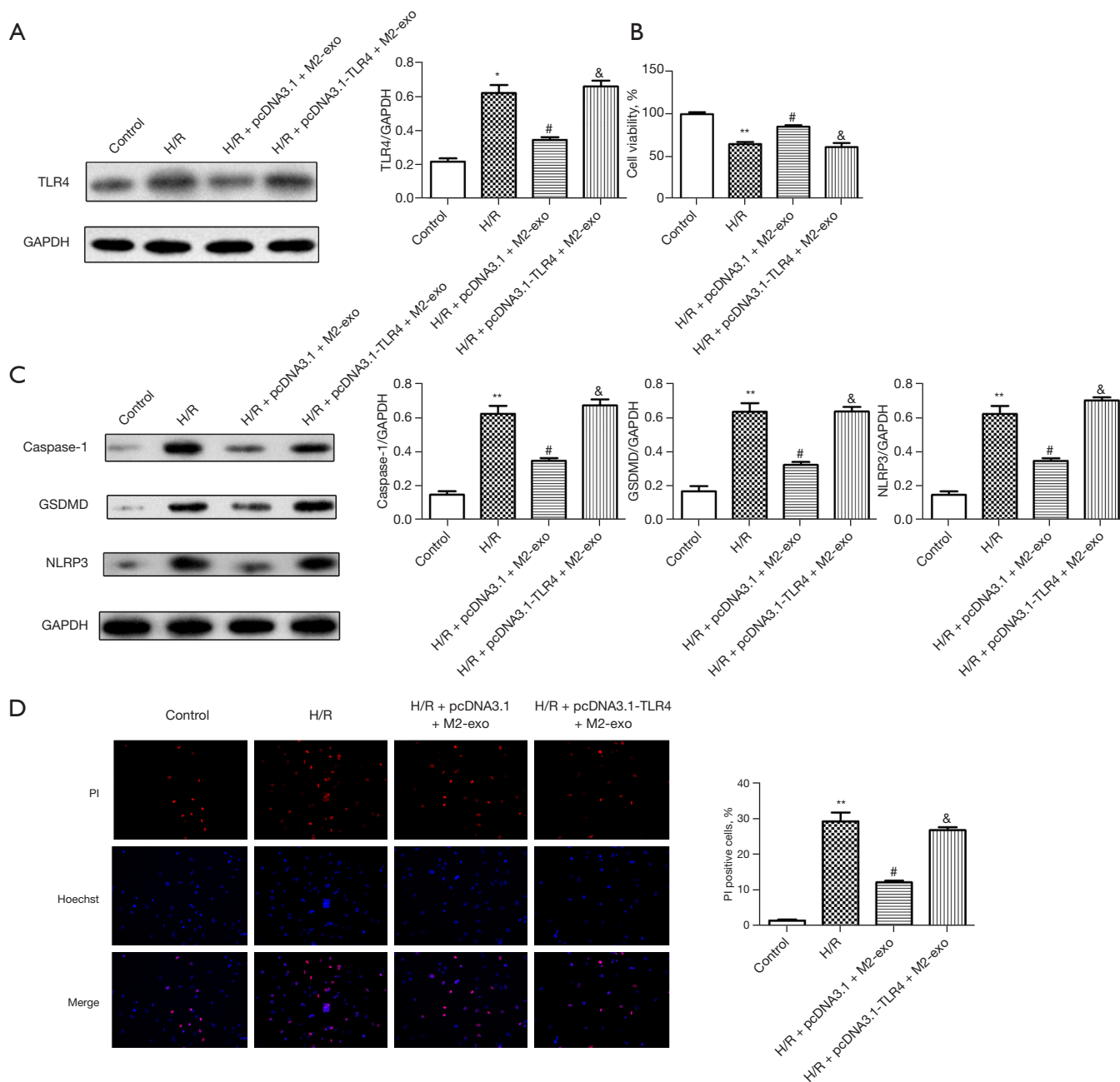


Figure 5 TLR4 overexpression reversed the protective effects of M2 exosomes in H/R-induced pyroptosis. (A) Western blot was used to assess the expression of TLR4. (B) Cell viability was detected using CCK-8. (C) The expression of caspase-1, GSDMD, and NLRP3 was detected by western blot. (D) The pyroptosis of the cells was detected by PI staining, 100x. *P<0.05, **P<0.01, vs. control group; #P<0.05, vs. H/R group; &P<0.05. TLR4, toll-like receptor 4; GAPDH, glyceraldehyde-3-phosphate dehydrogenase; H/R, hypoxia-reoxygenation; PI, propidium iodide; CCK-8, Cell Counting Kit 8.

the expression of TLR4 was significantly increased in the H/R group. However, the TLR4 expression levels were significantly downregulated in the H/R + pcDNA3.1 + M2

exosome group compared to the H/R group, and the TLR4 levels in the H/R + pcDNA3.1-TLR4 + M2 exosome group were increased compared to those in the H/R + pcDNA3.1 +

M2 exosome group. Based on the CCK-8 results (Figure 5B), we found that compared to the H/R group, the cell viability of the H/R + pcDNA3.1 + M2 exosome group was significantly enhanced. Cell activity was significantly inhibited in the H/R + pcDNA3.1-TLR4 + M2 exosome group. In addition, western blot was used to detect the expression of the pyroptosis-related proteins. The results (Figure 5C) showed that the expression of caspase-1, GSDMD, and NLRP3 was significantly downregulated in the H/R + pcDNA3.1 + M2 exosome group compared to the H/R group. The expression of caspase-1, GSDMD, and NLRP3 was significantly upregulated in the H/R + pcDNA3.1-TLR4 + M2 exosome group compared to the pcDNA3.1 + M2 exosome group. The immunofluorescence staining results (Figure 5D) showed that the PI positivity rate of the H/R + pcDNA3.1 + M2 exosome group was significantly lower than that of the H/R group; however, compared to the H/R + pcDNA3.1 + M2 exosome group, the PI positivity rate of the H/R + pcDNA3.1-TLR4 + M2 exosome group was significantly increased. In summary, we confirmed that TLR4 overexpression reversed the protective effect of M2 exosomes against H/R-induced pyroptosis.

Discussion

The gradual upgrading of medical technology has led to fruitful advances in treatment strategies for ischemic cardiovascular diseases. Thrombolytic therapy and adjunctive treatment with anti-platelet agents can partially restore blood supply and I/R injury exacerbates myocardial tissue necrosis. Several forms of cell death have been reported to accompany I/R injury (32,33), among which caspase-1-mediated pyroptosis has received widespread attention. In recent years, it has reported (34) that M2 macrophage-derived exosomes represent a potential treatment for myocardial I/R injury. In the present study, we found that M2 macrophage-derived exosomes carrying miR-145-5p significantly mitigated injury in H/R-induced cardiomyocytes. Our results confirmed that the M2 macrophage-derived exosome miR-145-5p targets and regulates the expression of TLR4 and inhibits pyroptosis in H/R-induced cardiomyocytes.

Exosomes of different origins can encapsulate signaling molecules and play regulatory roles in a variety of pathological disease processes (35,36). M2 macrophage-derived exosomes are closely associated with cellular processes, such as angiogenesis (37), cell proliferation,

and apoptosis (38). In addition, M2 macrophage-derived exosomes could deliver miRNAs to receptors that play the regulatory roles in tumors, pulmonary fibrosis, and cardiovascular disease. Li *et al.* found (39) that M2 macrophage-derived exosome miR-27a-3p promotes cancer stemness in HCC through the downregulation of thioredoxin-interacting protein (TXNIP). The overexpression of miR-328 by M2 macrophage-derived exosomes has been shown to exacerbate the development of pulmonary fibrosis by regulating the expression level of FAM13A (family with sequence similarity 13, member A) (40). It has been reported (34) that M2 macrophage-derived exosomes can carry miR-148a and alleviate MI/R injury by downregulating TXNIP and inhibiting the activation of the TLR4/NF- κ B/NLRP3 inflammasome signaling pathway. In our study, we showed that exosomes secreted by M2 macrophages improved H/R-induced cardiomyocyte activity. In addition, the western blot and immunofluorescence staining results confirmed that exosomes secreted by M2 macrophages partially reversed the pyroptosis in H/R-induced cardiomyocytes.

Myocardial I/R may be accompanied by a sustained inflammatory response, and inflammatory injury leads to the activation of the caspase-1-dependent programmed death pathway, also known as pyroptosis. Different from apoptosis, pyroptosis is dependent on the activation of caspase-1 by inflammasomes to mediate rapid cell death and promote inflammatory response. The immune system promotes the release of toll-like receptors (TLRs), tumor necrosis factor receptors, and other inflammatory factors during the initiation of pyroptosis. Xuan *et al.* (41) found that the long non-coding RNA Sox2OT binds to miR-23b, which affects the ability of the TLR4/NF- κ B signaling pathway to regulate pyroptosis, which in turn promotes myocardial injury. Trimetazidine has been reported (42) to attenuate myocardial I/R-induced pyroptosis by modulating the TLR4/MyD88 (myeloid differentiation factor 88)/NF- κ B/NLRP3 inflammatory pathway. Interestingly, we confirmed that TLR4 was a downstream target molecule of miR-145-5p. In addition, our results suggested that M2 macrophage-derived exosomes carrying miR-145-5p downregulate the level of TLR4 in H/R-induced cardiomyocytes. Additionally, M2 exosomes carrying miR-145-5p significantly inhibit the expression of GSDMD, NLRP3, and caspase-1 in H/R-induced cardiomyocyte. We hypothesized that the protective mechanism of the M2 macrophage-derived exosome miR-145-5p in myocardial injury is related to its targeted regulation of TLR4-

mediated pyroptosis.

Conclusions

In conclusion, our study confirmed that M2 macrophage-derived exosome miR-145-5p may play a protective role in myocardial I/R injury. We found that miR-145-5p targeted the regulation of TLR4 expression, inhibits pyroptosis, and mitigates H/R-induced myocardial injury. Our findings may lead to the development of a new therapeutic strategy for the treatment of myocardial I/R injury, and more specifically, to the development of an exosome-related targeted therapy. The main limitation of this study is the absence of *in vivo* experiments, which will be conducted in the future to verify the findings of this study.

Acknowledgments

We are grateful to all the participants for their contributions to the present study.

Funding: None.

Footnote

Reporting Checklist: The authors have completed the MDAR reporting checklist. Available at <https://atm.amegroups.com/article/view/10.21037/atm-22-6109/rc>

Data Sharing Statement: Available at <https://atm.amegroups.com/article/view/10.21037/atm-22-6109/dss>

Conflicts of Interest: All authors have completed the ICMJE uniform disclosure form (available at <https://atm.amegroups.com/article/view/10.21037/atm-22-6109/coif>). The authors have no conflicts of interest to declare.

Ethical Statement: The authors are accountable for all aspects of the work in ensuring that questions related to the accuracy or integrity of any part of the work are appropriately investigated and resolved. Our study was approved by the Hospital Ethics Committee and was conducted in accordance with the Declaration of Helsinki (as revised in 2013). The donors signed an informed consent form.

Open Access Statement: This is an Open Access article distributed in accordance with the Creative Commons Attribution-NonCommercial-NoDerivs 4.0 International

License (CC BY-NC-ND 4.0), which permits the non-commercial replication and distribution of the article with the strict proviso that no changes or edits are made and the original work is properly cited (including links to both the formal publication through the relevant DOI and the license). See: <https://creativecommons.org/licenses/by-nc-nd/4.0/>.

References

1. Lu D, Thum T. RNA-based diagnostic and therapeutic strategies for cardiovascular disease. *Nat Rev Cardiol* 2019;16:661-74.
2. Şahin B, İlgün G. Risk factors of deaths related to cardiovascular diseases in World Health Organization (WHO) member countries. *Health Soc Care Community* 2022;30:73-80.
3. Konijnenberg LSF, Damman P, Duncker DJ, et al. Pathophysiology and diagnosis of coronary microvascular dysfunction in ST-elevation myocardial infarction. *Cardiovasc Res* 2020;116:787-805.
4. Fernandez Rico C, Konate K, Josse E, et al. Therapeutic Peptides to Treat Myocardial Ischemia-Reperfusion Injury. *Front Cardiovasc Med* 2022;9:792885.
5. Pereira BLB, Rodrigue A, Arruda FCO, et al. Spondias mombin L. attenuates ventricular remodeling after myocardial infarction associated with oxidative stress and inflammatory modulation. *J Cell Mol Med* 2020;24:7862-72.
6. Tao L, Bei Y, Lin S, et al. Exercise Training Protects Against Acute Myocardial Infarction via Improving Myocardial Energy Metabolism and Mitochondrial Biogenesis. *Cell Physiol Biochem* 2015;37:162-75.
7. Duerr GD, Wu S, Schneider ML, et al. CpG postconditioning after reperfused myocardial infarction is associated with modulated inflammation, less apoptosis, and better left ventricular function. *Am J Physiol Heart Circ Physiol* 2020;319:H995-H1007.
8. Zhang M, Lei YS, Meng XW, et al. Igaratimod Alleviates Myocardial Ischemia/Reperfusion Injury Through Inhibiting Inflammatory Response Induced by Cardiac Fibroblast Pyroptosis via COX2/NLRP3 Signaling Pathway. *Front Cell Dev Biol* 2021;9:746317.
9. Zhang J, Huang L, Shi X, et al. Metformin protects against myocardial ischemia-reperfusion injury and cell pyroptosis via AMPK/NLRP3 inflammasome pathway. *Aging (Albany NY)* 2020;12:24270-87.
10. Cheng Y, Yang C, Luo D, et al. N-Propargyl Caffeamide Skews Macrophages Towards a Resolving M2-Like

- Phenotype Against Myocardial Ischemic Injury via Activating Nrf2/HO-1 Pathway and Inhibiting NF- κ B Pathway. *Cell Physiol Biochem* 2018;47:2544-57.
11. Cheng Y, Feng Y, Xia Z, et al. ω -Alkynyl arachidonic acid promotes anti-inflammatory macrophage M2 polarization against acute myocardial infarction via regulating the cross-talk between PKM2, HIF-1 α and iNOS. *Biochim Biophys Acta Mol Cell Biol Lipids* 2017;1862:1595-605.
 12. Qi Y, Jin C, Qiu W, et al. The dual role of glioma exosomal microRNAs: glioma eliminates tumor suppressor miR-1298-5p via exosomes to promote immunosuppressive effects of MDSCs. *Cell Death Dis* 2022;13:426.
 13. Sohrabi B, Dayeri B, Zahedi E, et al. Mesenchymal stem cell (MSC)-derived exosomes as novel vehicles for delivery of miRNAs in cancer therapy. *Cancer Gene Ther* 2022;29:1105-16.
 14. Li H, Luo Y, Liu P, et al. Exosomes containing miR-451a is involved in the protective effect of cerebral ischemic preconditioning against cerebral ischemia and reperfusion injury. *CNS Neurosci Ther* 2021;27:564-76.
 15. Zhou T, Zhang M, Xie Y, et al. Effects of miRNAs in exosomes derived from α -synuclein overexpressing SH-SY5Y cells on autophagy and inflammation of microglia. *Cell Signal* 2022;89:110179.
 16. Tkach M, Théry C. Communication by Extracellular Vesicles: Where We Are and Where We Need to Go. *Cell* 2016;164:1226-32.
 17. Leoni G, Neumann PA, Kamaly N, et al. Annexin A1-containing extracellular vesicles and polymeric nanoparticles promote epithelial wound repair. *J Clin Invest* 2015;125:1215-27.
 18. Zhang X, Deeke SA, Ning Z, et al. Metaproteomics reveals associations between microbiome and intestinal extracellular vesicle proteins in pediatric inflammatory bowel disease. *Nat Commun* 2018;9:2873.
 19. Henning RJ. Cardiovascular Exosomes and MicroRNAs in Cardiovascular Physiology and Pathophysiology. *J Cardiovasc Transl Res* 2021;14:195-212.
 20. Yang X, Cai S, Shu Y, et al. Exosomal miR-487a derived from m2 macrophage promotes the progression of gastric cancer. *Cell Cycle* 2021;20:434-44.
 21. Zhang Z, Hu J, Ishihara M, et al. The miRNA-21-5p Payload in Exosomes from M2 Macrophages Drives Tumor Cell Aggression via PTEN/Akt Signaling in Renal Cell Carcinoma. *Int J Mol Sci* 2022;23:3005.
 22. Long R, Gao L, Li Y, et al. M2 macrophage-derived exosomes carry miR-1271-5p to alleviate cardiac injury in acute myocardial infarction through down-regulating SOX6. *Mol Immunol* 2021;136:26-35.
 23. Chen H, Gao J, Xu Q, et al. MiR-145-5p modulates lipid metabolism and M2 macrophage polarization by targeting PAK7 and regulating β -catenin signaling in hyperlipidemia. *Can J Physiol Pharmacol* 2021;99:857-63.
 24. Zhou W, Ji L, Liu X, et al. AIFM1, negatively regulated by miR-145-5p, aggravates hypoxia-induced cardiomyocyte injury. *Biomed J* 2022;45:870-82.
 25. Li Y, Tian Z, Tan Y, et al. Bmi-1-induced miR-27a and miR-155 promote tumor metastasis and chemoresistance by targeting RKIP in gastric cancer. *Mol Cancer* 2020;19:109.
 26. Wang K, Wang X, Zou J, et al. miR-92b controls glioma proliferation and invasion through regulating Wnt/ β -catenin signaling via Nemo-like kinase. *Neuro Oncol* 2013;15:578-88.
 27. Rios FJ, Touyz RM, Montezano AC. Isolation and Differentiation of Human Macrophages. *Methods Mol Biol* 2017;1527:311-20.
 28. Ma YS, Wu TM, Ling CC, et al. M2 macrophage-derived exosomal microRNA-155-5p promotes the immune escape of colon cancer by downregulating ZC3H12B. *Mol Ther Oncolytics* 2021;20:484-98.
 29. Xie H, Yao J, Wang Y, et al. Exosome-transmitted circVMP1 facilitates the progression and cisplatin resistance of non-small cell lung cancer by targeting miR-524-5p-METTL3/SOX2 axis. *Drug Deliv* 2022;29:1257-71.
 30. Zhang B, Mao S, Liu X, et al. MiR-125b inhibits cardiomyocyte apoptosis by targeting BAK1 in heart failure. *Mol Med* 2021;27:72.
 31. Zhang B, Sun C, Liu Y, et al. Exosomal miR-27b-3p Derived from Hypoxic Cardiac Microvascular Endothelial Cells Alleviates Rat Myocardial Ischemia/Reperfusion Injury through Inhibiting Oxidative Stress-Induced Pyroptosis via Foxo1/GSDMD Signaling. *Oxid Med Cell Longev* 2022;2022:8215842.
 32. Stamenkovic A, O'Hara KA, Nelson DC, et al. Oxidized phosphatidylcholines trigger ferroptosis in cardiomyocytes during ischemia-reperfusion injury. *Am J Physiol Heart Circ Physiol* 2021;320:H1170-84.
 33. Xia Y, He F, Moukeila Yacouba MB, et al. Adenosine A2a Receptor Regulates Autophagy Flux and Apoptosis to Alleviate Ischemia-Reperfusion Injury via the cAMP/PKA Signaling Pathway. *Front Cardiovasc Med* 2022;9:755619.
 34. Dai Y, Wang S, Chang S, et al. M2 macrophage-derived exosomes carry microRNA-148a to alleviate myocardial ischemia/reperfusion injury via inhibiting TXNIP and the

- TLR4/NF- κ B/NLRP3 inflammasome signaling pathway. *J Mol Cell Cardiol* 2020;142:65-79.
35. Miao C, Wang X, Zhou W, et al. The emerging roles of exosomes in autoimmune diseases, with special emphasis on microRNAs in exosomes. *Pharmacol Res* 2021;169:105680.
 36. Tian Y, Cheng C, Wei Y, et al. The Role of Exosomes in Inflammatory Diseases and Tumor-Related Inflammation. *Cells* 2022;11:1005.
 37. Yang Y, Guo Z, Chen W, et al. M2 Macrophage-Derived Exosomes Promote Angiogenesis and Growth of Pancreatic Ductal Adenocarcinoma by Targeting E2F2. *Mol Ther* 2021;29:1226-38.
 38. Yin Z, Zhou Y, Ma T, et al. Down-regulated lncRNA SBF2-AS1 in M2 macrophage-derived exosomes elevates miR-122-5p to restrict XIAP, thereby limiting pancreatic cancer development. *J Cell Mol Med* 2020;24:5028-38.
 39. Li W, Xin X, Li X, et al. Exosomes secreted by M2 macrophages promote cancer stemness of hepatocellular carcinoma via the miR-27a-3p/TXNIP pathways. *Int Immunopharmacol* 2021;101:107585.
 40. Yao MY, Zhang WH, Ma WT, et al. microRNA-328 in exosomes derived from M2 macrophages exerts a promotive effect on the progression of pulmonary fibrosis via FAM13A in a rat model. *Exp Mol Med* 2019;51:1-16.
 41. Xuan L, Fu D, Zhen D, et al. Long non-coding RNA Sox2OT promotes coronary microembolization-induced myocardial injury by mediating pyroptosis. *ESC Heart Fail* 2022;9:1689-702.
 42. Chen X, Lin S, Dai S, et al. Trimetazidine affects pyroptosis by targeting GSDMD in myocardial ischemia/reperfusion injury. *Inflamm Res* 2022;71:227-41.

(English Language Editor: L. Huleatt)

Cite this article as: Wei L, Zhao D. M2 macrophage-derived exosomal miR-145-5p protects against the hypoxia/reoxygenation-induced pyroptosis of cardiomyocytes by inhibiting TLR4 expression. *Ann Transl Med* 2022;10(24):1376. doi: 10.21037/atm-22-6109